



UNIVERSITÀ  
DEGLI STUDI  
FIRENZE

# FLORE

## Repository istituzionale dell'Università degli Studi di Firenze

### Investigation of a pure hydrogen fueled gas turbine burner

Questa è la Versione finale referata (Post print/Accepted manuscript) della seguente pubblicazione:

*Original Citation:*

Investigation of a pure hydrogen fueled gas turbine burner / Cappelletti, Alessandro; Martelli, Francesco. - In: INTERNATIONAL JOURNAL OF HYDROGEN ENERGY. - ISSN 0360-3199. - ELETTRONICO. - 42:(2017), pp. 10513-10523. [10.1016/j.ijhydene.2017.02.104]

*Availability:*

This version is available at: 2158/1080338 since: 2017-05-03T10:45:32Z

*Published version:*

DOI: 10.1016/j.ijhydene.2017.02.104

*Terms of use:*

Open Access

La pubblicazione è resa disponibile sotto le norme e i termini della licenza di deposito, secondo quanto stabilito dalla Policy per l'accesso aperto dell'Università degli Studi di Firenze (<https://www.sba.unifi.it/upload/policy-oa-2016-1.pdf>)

*Publisher copyright claim:*

(Article begins on next page)

Alessandro Cappelletti, Francesco Martelli, Investigation of a pure hydrogen fueled gas turbine burner, International Journal of Hydrogen Energy, Available online 11 March 2017, ISSN 0360-3199, <http://dx.doi.org/10.1016/j.ijhydene.2017.02.104>.  
(<http://www.sciencedirect.com/science/article/pii/S0360319917306122>)

## **Investigation of a pure hydrogen fueled gas turbine burner**

**Alessandro Cappelletti <sup>1\*</sup>, Francesco Martelli <sup>2</sup>**

<sup>1</sup> CREAR-DIEF Università degli Studi di Firenze, Via S. Marta, 3 - 50139 Florence – Italy

\*Corresponding Author's Information:

Eng. Alessandro Cappelletti, PhD

CREAR - Department of Industrial Engineering (DIEF)

Università degli Studi di Firenze, Via S. Marta, 3 - 50139 Florence – Italy

Email: [alessandro.cappelletti@unifi.it](mailto:alessandro.cappelletti@unifi.it)

## Abstract

Hydrogen can represent an option for a low emission gas turbine if low NO<sub>x</sub> combustion systems are developed. This paper describes the design and the investigations carried out on a lean premixed burner 100% hydrogen supplied. An existing heavy-duty gas turbine burner was modified with a new axial swirler and a co-flow injection system. The designed prototype presents the interesting feature where the variable premixing level permits a wide-ranging case studying. The burner prototype was investigated during a test campaign performed on an atmospheric test rig. Flame control on burner prototype, fired by pure hydrogen, was achieved by managing the premixing degree and the flow velocity. NO<sub>x</sub> emissions, flash-back limit, and burner pressure drop were measured over a wide range of the main operating parameters: equivalence ratio, premixer discharge velocity and thermal input. Results of the measurements outline as higher velocity flow (depending on the burner arrangements and operating conditions) is necessary to avoid flame positioning inside the premixer duct when hydrogen is used. The best arrangement can limit the NO<sub>x</sub> emissions to 17ppm but with an outlet velocity about 120m/s. The numerical activity integrates the information on the flame shape, and it improves the knowledge of the NO<sub>x</sub> emissions and their chemical path. Anyway, the study confirmed the operability of the system and great perspective regarding NO<sub>x</sub> emission containment.

Keywords: Hydrogen, Gas Turbine, Premixed Flame, NNH, NO<sub>x</sub>, experiment

## Nomenclature

c	progress variable	[-]
D	premixer outlet diameter	[m]
k	turbulent kinetic energy	[m <sup>2</sup> /s <sup>2</sup> ]
Sw	Swirl number	[-]
T	temperature	[K]

CFD	Computational Fluid Dynamics
DLN	Dry Low NO <sub>x</sub>
IGCC	Integrated Gasification Combined Cycle
NO <sub>x</sub>	Nitro Oxide
PDF	Probability Density Function

RANS	Reynolds Averaged Navier Stokes
SST	Shear Stress Models
STD	Standard Deviation
TAO	Turbogas Accesso Ottico – Turbogas Optical Entry
MGT	Micro Gas Turbine

## Greek

$\omega$	specific turbulent dissipation	[1/s]
$\phi$	equivalent ratio	[-]

## I. Introduction

The hydrogen is an important driver for the future energy scenario [1,2] because the combustion of hydrogen eliminates the direct generation of carbon, but its production and using is not already carried out for an industrial and commercial application at 100% H<sub>2</sub>. The gas turbine is a viable alternative to fuel cell technology regarding reliability [3], expected lifetime and cost. They permit to use hydrogen with a considerable level of impurity as CO; so it is possible to increase in value many solid wastes (municipal wastes, sewage sludge, meat and bone meal, etc.) [4–6] or carbon-based fuels that could be used to produce a hydrogen-rich syngas. The Fusina project [7] started for the using of the hydrogen from the petrochemical facilities of Porto Marghera (Italy). In this contest, the recent technology also gives the possibility to use an abundant energy source like coal, in a clean system with high efficiency (IGCC) [8] with net CO<sub>2</sub> cycles [9,10]. Even though gas turbine is a well-established technology for low hydrogen syngas but the operation on pure hydrogen is still a challenging frontier. The combustor is the only component of a gas turbine that requires major redesign effort for operation on 100% hydrogen, due to the fuel characteristics [11,12]. However, the use of hydrogen as a fuel is nowadays limited to gas turbines equipped by diffusion flame combustors [13–15], where the pure hydrogen supply leads to NO<sub>x</sub> emissions about three times higher than in the case of natural gas firing [16]. Methods for reducing pollutant emissions are borrowed from those used in diffusive gas turbine combustion chambers supplied by natural gas. The experience from DLN gas turbine combustor suggests the premix combustion as a useful method to control NO<sub>x</sub> emission, but in the case of 100% hydrogen combustion, this technology is not yet mature.

The literature shows the main difference between hydrogen respect the natural gas. Shelil et al. [17], Kwon [18], Rozenchan [19] and Pareja et al. [20] report the very high laminar flame speed. Noble et al. [21] report the tendency to a very quick flashback, where the limited progress time does not permit a right management of this phenomena.

The flame speed is the main element for all premixed flames because it defines the position of the flame front and the behavior about the flashback is the main problem for the premixed combustion

chamber. Schönborn et al. [22] show a very short ignition delay time of the hydrogen flames and how the increasing of Reynolds cause a reducing of the delay. This behavior needs a high flow velocity to prevent flash-back phenomena, with obvious negative repercussions on combustor pressure drop. During the last decade, several studies on hydrogen-fueled premixed combustors have been carried out. Burmberger et al. [23] show an experimental activity the possibility, by proper vortex breakdown, to obtain stable flame anchored close to the exit of the nozzle on a radial swirler burner prototype. In this case, the burner exhibited remarkable fuel flexibility, and the flashback phenomena were reasonably controlled. Therkelsen et al. [24] study some modifications to the fuel injectors system of a commercial MGT to allow a pure H<sub>2</sub> operability. These changes were focused on achieving three different fuel/air mixing profiles while maintained similar equivalence ratio operational ranges; as other cases, the engine fueled with hydrogen produced larger volumes of NO<sub>x</sub>. Other innovative technologies are described in the literature, for example, the Micro-mixing [25], the Multi-Tube Mixing [26] or the Lean Direct Injection [27]. These designs are characterized by the using of small passage as a premixing duct to reduce the flashback and improvement the NO<sub>x</sub> production control, but all this solution is far to a great operability with pure hydrogen in a gas turbine.

In this context, the present work describes the experimental and the numerical analysis on a premixer prototype derived from a natural gas industrial unit. The design idea was to reduce the distance with the real gas turbine combustor. The premixer was tested at ENEL's TAO test facility in Livorno (Italy). The tests were performed for natural gas, methane/hydrogen mixture, and pure hydrogen too. The design activity and the preliminary experimental data are reported in Brunetti et al. [28], which are focused on the effect of hydrogen content on the main operating parameters. The aim of this paper is the investigation of the pure H<sub>2</sub> fueling because in literature deep analyses on only this condition are few also for the other cases, as in Galletti et al. [29] and York et al. [26].

## **II. The investigated object**

The prototype derives from a TG50 DLN combustor installed on a heavy duty gas turbine. The initial premixer was featured by an axial swirler and cross-flow fuel injection system [30,31]. Eight blades compose the swirler, but it is not able to produce a stable toroidal recirculation zone at premixer's outlet [32]. A new swirler by a wider mean outlet angle (43°,  $Sw=0.7$ ) was designed and built in order the suggestion from Lilley [33] and Burmberger et al. [23].

The injection system is modified to be co-flow, and it is inspired by Therkelsen [34]. Its design philosophy is the preventing the high turbulence regions, typical of the cross-flow, which brings to the flashback.

The injection system is composed by eight lances which pierce the swirler blades, see Figure 1. The main feature of the injection system is the possibility to move along the axial direction so the fuel delivery point can change as well as the mixing level. However, the moving is possible only when the unit is cold and shut-down, so it is not an active system. This solution is a good adjustment because of the experience from Cerutti et al. [35] shows the modification of premixing level needs a complete rearrangement of the test rig.

To extend the operating range and to simplify the operating a commercial pilot burner was installed on the premixer axis. The schematic drawing in Figure 1 shows the main components of the developed burner prototype.

The operative condition range of the burner prototype, see Table 1, was based on the premixer equivalent ratio, air temperature of the original TG50 DLN premixing system operated at full-load with natural gas, but it is modified in according with the experienced obtained from the experimental activity.

### **III. Test facility**

The combustion test rig - named TAO (Figure 2) - was installed in the ENEL's experimental area located in Livorno (Tuscany, Italy). This facility was built in 2004 with the aim to perform experimental investigations on gas turbine burners using advanced optical diagnostic techniques. Among several experimental campaigns performed up to now on this facility. Many of this study were focused on the analysis of thermo-acoustic combustion instabilities in the lean premixed burners and a part of results are reported in Tiribuzi et al. and Cipriano et al. [36,37]. The rig consists of a vertical atmospheric combustion chamber; the maximum thermal input is 800 kW. Figure 2 shows a sectional view of the tested burner installed on the rig. On four walls of the octagonal chamber, there are installed flat quartz windows used for optical access. The stainless steel chamber is 85 cm long with a 31 cm equivalent inner diameter ( $2 \cdot r_c$ , see Figure 2). At its end, a conical shaped restriction leads to a downstream smaller chamber used for gas sampling and separates the combustion chamber from the exhaust discharge piping. About the tests described here, premixed and pilot gas lines were used to supply the main and the pilot burner respectively. Air is provided to the combustion chamber using two different lines. The first one is connected to the main fan and carries heated air to the plenum upstream of the main burner. The other supplies the pilot burner with air at ambient temperature. For technical characteristics of the pilot, it was fueled only with natural gas even in a case with hydrogen fueling. The combustion test rig is equipped with resident instrumentation, dedicated to air and fuel systems' control and necessary to ensure proper test rig operation. For test execution, the main instruments are those providing mass flow measurements. Fuel mass flows have been measured using both standard orifices and flow meters. Pressure and temperature transmitters provide continuous monitoring of air and fuel supply conditions. The test hardware has been equipped with dedicated instrumentation to provide a detailed and comprehensive screening of the combustion system performances. Flue gas temperature inside the combustion chamber was measured using twelve thermocouples Pt-Rd type, installed in the chamber at a radial distance of 51 mm (equivalent to  $0.75 D$ ) from the burner axis (see " $r_t$ " in Figure 2 for details). Two 180 degree-shifted thermocouples were installed at the burner exit to monitor its metal temperature and to identify the flame flashback onset. Two sampling probe and a thermocouple were installed at the combustion chamber exit for measuring main species and flue gas temperature. NO<sub>x</sub> emissions were measured using both chemiluminescence and infrared analyzers; this unit gave  $\pm 1$  ppm in accuracy. Each test day it was calibrated with a certificated gas mixture. The flame pattern has been obtained using the OH\* chemiluminescence imaging. The OH\* emission imaging highlights specific zones where heat release rates are supposed to be highest and carries out morphological and dynamic information of the flame. The data acquisition of the test rig is performed by an electronic system that reads and stores the data from each sensor with 1 Hz frequency; the values are also visualized in real time. The mean values for each single test point were evaluated by averaging 30 consecutive acquisitions and checking the minimum, maximum and the STD values of this value set.

### **Correction temperature value**

The data collected by thermocouples needs to be corrected by using a correlation to take into account of their radiation energy losses. When a thermocouple is in a high-temperature zone, as in a flame, the radiation losses are significant, so the measured value is lower than the actual flow value. The difference can be over 200K in the higher temperature zone. The equation 1, proposed by Kaskan [38], evaluates the  $\Delta T$  between the actual flow value and the measured one.

$$\Delta T_{rad} = \frac{1.25 \varepsilon \sigma T_w^4 D^{0.75}}{\lambda} \left( \frac{\eta}{\rho v} \right)^{0.25} \quad 1$$

- $\eta$       viscosity of air
- $\rho v$     mass flow
- $\lambda$       thermal conductivity of air
- $\sigma$       Stefan-Boltzmann constant
- $\varepsilon$       constant = 0.22
- $T_w$     temperature measured by the thermocouples

Figure 3 reports the comparison between the measured values and the corrected ones, the difference for temperature over 1000K is about from 130 to 180 Kelvin. For the values of viscosity and thermal conductivity were used the temperature depended on values of the air from an open database. The main issue of this equation is the “ $\rho v$ ” mass flow evaluating because without a CFD simulation is impossible knowing the local value, for the investigated case. An analysis of same reactive CFD simulations reports a constant value for “ $\rho v$ ” along the measuring profile for each case.

#### IV. Numerical approach

The numerical simulation is performed to deepen some details imperceptible from the experimental test. The hydrogen flames are invisible to naked eye and OH\* emissions provide only a bi-dimensional flame shape, but the information from the natural gas direct observation [28] suggests a complex shape started from the eight lances.

Another important aspect is the NOx emission and the understanding which chemical paths are more influence on global emissions. Gas turbine combustion simulation requires taking into account the interaction between chemistry and turbulence. Gobbato et al. [39] show a low computational cost numerical approach, but it could be used only for a diffusion flame. Looking at the test case under investigation, the air/fuel mixture produced by the interaction between the air and the fuel is not homogeneous at the combustion chamber inlet. A partial premix model based on the Zimont approach [40,41] in conjunction with the Steady Laminar Flamelet Model of Peters [42,43], with Non-equilibrium and Non-adiabatic PDF tables, was selected. The code uses directly fitted curves of the laminar flame speed obtained from numerical simulations proposed by Gottgens et al. [44]. A RANS approach was used for turbulence modeling, and the k- $\omega$  SST model was selected as suggested

in some work on gas turbine combustion chamber [45–47]. The laminar flamelet tables were generated by using the kinetic mechanism proposed by Li et al. [48,49], this mechanism is suggested by Ströhle et al. [50] because it is optimized for the hydrogen combustion in atmospheric condition. The following numerical results were obtained with CFD simulations carried out with ANSYS FLUENT code (ver. 14.5) [51,52], where the main governing equation are:

$$1) \text{ Mass conservation: } \frac{\partial(\rho)}{\partial t} + \text{div}(\rho u) = 0 \quad 2$$

$$2) \text{ Momentum: } \frac{\partial(\rho u)}{\partial t} + \text{div}(\rho u u) = -\text{grad}(p) + \text{div}(\tau) + F \quad 3$$

$$3) \text{ Energy: } \frac{\partial(\rho E)}{\partial t} + \text{div}[u(\rho E + p)] = \text{div}[k_{eff} \nabla T - \sum_j h_j J_j] + S_h \quad 4$$

$\rho$	density
$p$	static pressure
$t$	time
$u$	velocity vector
$\tau$	viscous stress
$F$	body force vector
$E$	energy per unit mass
$k_{eff}$	heat transfer coefficient
$h_j$	enthalpy
$S_h$	energy source

Regarding the numerical accuracy of the code, all information are available from the software house with the code verification manual [53].

The simulations were performed using a second order discretization for all the equations because it permits to increase the accuracy of the results on a tetraedical mesh, as reported on Fluent manual [51,52]. The boundary conditions were imposed regarding inlet total pressure and outlet static pressure volume and finally the actual mass flow rate is checked. On the combustion chamber walls, a uniform temperature is imposed to evaluate the cooling of the test rig. The convergence accuracy of the simulations was performed by checking the equations residual and the value of some specific variables. The calculation was stopped if the residual values became lower than  $10^{-6}$  and it was



constant for the 1.000 following iterations. The monitored quantities were the average temperature and fuel mass fraction at the outlet.

### **Post processor for emission evaluation**

NO<sub>x</sub> chemistry is too slow to be accurately represented by the laminar flamelet model; thus a specific postprocessor is required for their accurate evaluation. The first used tool works on the reactive simulations results, and it resolves one transport equation for the pure thermal path. NO<sub>x</sub> chemistry and turbulence interaction were modeled using assumed shape PDF distributions of temperature. The validation of the model was performed on many cases of gas turbine combustors [16,54–56].

In hydrogen flames generally, only the NO<sub>x</sub> production from the Zeldovich and N<sub>2</sub>O mechanisms are considered. Skottene et al. [57] report the importance of the NNH [58,59] way for the NO production in a hydrogen flame. So this study uses also a new post-processor available on ANSYS FLUENT ver. 14.5 [52]. It is not a network reactor post-processor but it uses transport equations.

This tool is based on a stiff solver where a detailed kinetic was imported and elaborated on all mesh cells. The tool can resolve many reactions, with low computational cost because the aerodynamics is frozen. For this analysis the Gri-mech 3.0 [60] was selected, this mechanism is used in many works about the analysis of NO<sub>x</sub> emissions [57,61–63]. The postprocessor uses the temperature and all original species fields from the previous reactive simulation. For this reason, the original simulation had to be resolved with kinetics that didn't include the pollutant species, as the selected Li et al. [48]. A specific transport equation resolves each pollutant species. All un-pollutant species, in the detailed kinetic and not in the original simulation, are evaluated by a chemical equilibrium calculation at the fixed temperature of the original solution. The Gri-mech was developed for hydrocarbon fuels. Thus it includes species and reaction with carbon; the solver eliminates all these elements because they are unnecessary.

### **Solid model and computational mesh**

Figure 4 shows a view of the premixer and the combustion chamber geometric model with details about the air and fuel inlet. The original periodicity of 45° was extended to 90° to avoid the influence on the solution. The computational mesh is hybrid non-structured, and it was generated by the commercial code Centaur™ [64]. The grid is composed of prismatic layers used for near-wall treatment and tetrahedral cells elsewhere.

The mesh independency is investigated from a coarser (2.0M) to the fine grid (6.0M). The last three case 4.4M, 5.0M, and 6.0M present the same results, so the 4.4M was selected for the numerical investigation.

## **V.Experimental result**

The experimental activity is carried out mainly on two setups. The first investigate the maximum premixing level with the pilot torch turn-off, and it is defined as the nominal case.

A lower premixing level characterizes the second configuration; the injection points were collocated half distance from the outlet. In this setup, the pilot torch was maintained on.

### Gas temperature distribution

The effect of the hydrogen content, thermal input, flow condition and mixing level on the gas temperature distribution along the combustion chamber was estimated using in-flame thermocouple measurement. The temperature profiles are reported in non-dimensional, defined by equation 5:

$$T_{x-dimensionless} = \left( \frac{T_x}{\phi} - \frac{T_0}{\phi} \right) / T_{ref} \quad 5$$

$T_x$ : Temperature of X thermocouple

$T_0$ : Inlet air temperature

$T_{ref}$ : Reference Temperature = 1[K]

### Equivalence ratio and Thermal input effects

The first explored set up was the case with the greatest premix level, for a safety operating the airflow rate had to be increased to about 128-130 m/s. From this safe condition, the test explored the variation of gas flow rate with the fixed airflow rate. This experimental setup permits to analyze the effect of the equivalence ratio thus thermal input on the flame shape. Figure 5 reports the temperature in non-dimensional form and the profiles depend upon the equivalence ratio  $\Phi$ . The reported profiles are quite overlapped, so the flame shape is not influenced by the equivalence ratio and thermal input. This result confirms the general roles of premixed combustion system that the flame shape is mainly controlled by the aerodynamic.

### Airflow effect

The second case was a low premix configuration with the nominal thermal input, 130 kW. The premix outlet velocity is the variable quantity with a range from 84 to 122 m/s. This data set is reported with the same non-dimensional analysis, but the data population was divided into two groups: the values higher 100 m/s and the lower ones. The Figure 6A and the Figure 7A report the non-dimension analysis for each data groups. The cases with velocity over 100 m/s the flame present a pattern opener than the other cases; the next elaboration empathizes this result. The analyzed X/D range is limited from 0.3 to 6.3, and the average values for each data groups is evaluated. The Figure 6B and the Figure 7B show the results with their trend lines. The line of over 100 m/s cases is second order polynomial but the lower 100 m/s cases one is a third order polynomial.

In this case, the airflow manages the flame shape with a significant influence because over 100m/s the toroidal recirculation zone is very big. In lower velocity cases, the recirculation zone is compact.

### Pollutants

In hydrogen fueling the only emissions are nitrous oxides and the current experience in operative gas turbine [7,16] reports high values, incompatibles with existing regulations. During the experimental activities, the NOx emissions were measured for each explored configuration as the

other quantities. The upper graph of Figure 8A shows the NO<sub>x</sub> emissions measured for the first analyzed case: constant the airflow rate and equivalence ratio changing.

For this set of data, NO<sub>x</sub> emissions are quite low from 6 up to 17 ppm @15%O<sub>2</sub>. In fact, this configuration is characterized by nominal premixing and pilot flame switched off. On the other side, the effect of the equivalence ratio is quite strong, about +11 ppm NO<sub>x</sub> for equivalence ratio from 0.258 to 0.338 (+13.7 ppm each +0.1 of  $\phi$ ) and the thermal input from 155 to 207 kW.

The graph of Figure 8B reports the low premixing configuration, with pilot switched on, and the airflow rate changes the equivalence ratio. The chart also reports the outlet velocity to emphasize the flow rate effect. In this case, measured NO<sub>x</sub> emission were much higher due to the pilot contribution and to the poorest air/fuel mixing. The relation between NO<sub>x</sub> and equivalence ratio is about linear with a rate of +24.7 ppm each +0.1 of  $\phi$ . Briefly considering all the configurations tested, the flame shape effect on the NO<sub>x</sub> emission is limited. The main driver is the combination of the premixing level and equivalent ratio.

In all cases the NO<sub>x</sub> emissions are quite low, from 5 up to 38 ppm@15%O<sub>2</sub>), also keeping in mind that combustion chamber rig is non-adiabatic.

### **Operability**

The flashback limit was investigated by changing step-by-step both the air and the fuel flow rate (keeping the equivalent ratio unchanged  $\phi=0.22$ ) until the flashback was detected. Flashback onset was detected via UV camera signal that slightly anticipated the facility shut-down driven by the burner overheating protection. The protection is activated when the difference between the burner metal temperature and the combustion air temperature was larger than 15°C. We observed flashback was generally a mix between core flashback and boundary layer, but the second generated on the pilot burner.

The investigations were performed for both arrangements nominal and low premix, and the results are shown in Table 2. The nominal configuration for a stable burner operation needs 127 m/s discharge velocity. In the case of low premixing the limit discharge velocity decreases down to 87 m/s, but in this case the pilot was switched on. The higher burner exit velocity is required to prevent flashback phenomena led to a significant increase of the burner pressure drop, see Table 2. The nominal configuration presents a 6% pressure drop; a turbine required a value lower than 4% otherwise its performance decrease excessively.

## **VI.Numerical results**

This paragraph reports the comparison with the experimental data and other interesting information that only the numerical procedure can show. The selected point is a low premixing case, but the torch pilot was switched off. The pilot is natural gas fueled and it is a problem for the numerical code because it is not able to analyze two different fuels. The boundary condition of this case are reported in Table 3. Figure 9A shows the comparison between experimental data and CFD, in non-dimensional form. The dotted line in Figure 9B shows the position of thermocouples as compared with the flame.

The numerical results present an acceptable agreement with the experimental ones. The trend of the flame shape is the same: a third order polynomial characterizes it.

The main difference is near the metal wall, where the CFD results are higher of 10% than the experimental. The test rig was cold, but the cooling distribution was not well known, probably the heat exchange is more intense near the premixer where there is the air plenum. The uniform condition of the wall temperature used in the simulation is too limited.

Figure 9B shows the CFD temperature field in a longitudinal plane. The zone with a high temperature ( $>2000\text{K}$ ) is little and compact; this condition influences the NO emission.

The experimental measuring shows a low value for the in-flame temperature, in fact, the thermocouples position line is tangent with the high-temperature zone.

Figure 10 shows the experimental  $\text{OH}^*$  image, from [28], and the Premix - C rate field in a longitudinal plane. The two images represent a similar information on the flame position but using a different visualization method. The flame position is well identified, and the shape is similar in the same visible zone.

### *1. Actual flame shape*

The experimental image shows only a limited region of the flame, for example, it is not able to show what happens in the premixer, but the CFD can it.

Figure 11 shows the complete flame shape; the flame is in the duct, and the flame ignition is very close to the injection point. The metal walls are not involved by the flame because the cold air slot protects them. The  $\text{OH}^*$  chemiluminescence image was not able to show what happened in the duct. The flashback detection system in this operative condition did not report flashback; probably it was influenced by the cold airflow from the slot. The early ignition does not permit the correct mixing; the flame shape is very similar to a stretched diffusion flame ignited from each lance; the flame front is the boundary of gas with the air. This un-mixing condition exists with  $84\text{ m/s}$  discharge velocity and a high swirling component.

### *2. NO emission*

The NO is the only emission in the hydrogen combustion thus, its evaluation is important. In this study, three evaluation ways were considered: the pure Zeldovich postprocessor, the decoupled limited to only the Zeldovich path and the decoupled with a complete chemistry. This approach is similar to the work of Guo et al. [65] where the analyses were repeated with limited chemistry to emphasize the contribution of a specific path. Table 4 reports the results, the value from the Decoupled post processor, with complete chemistry, is very close to the experimental value,  $41\text{ ppm NO @15\% O}_2$  vs.  $38\text{ ppm NO @15\% O}_2$ . The other two cases, where the only thermal path was evaluated, present a very low value as the temperature field suggest. This result plainly shows the thermal isn't the main way for the NO emission for this flame but the NNH [58,59] way is the main cause.

The NNH way is significant when a high concentration of dissociated  $\text{H}_2$  and  $\text{O}_2$  are present in the flame; this is typical for the hydrogen combustion in air. The high level of H promotes the R1 reaction, and the O promotes the R2 reaction with final NO production.

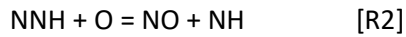


Figure 12 stress this result reporting the iso-surface of reaction rate for the thermal way and the NNH way (R2). The volume influenced by the thermal way is smaller than the NNH ones in accord with the global production value. The main information from Figure 12 is about the early starting of the production from NNH, in the initial part of the flame. Near the injection point where the temperature is very low and where the fuel presents the maximal concentration. The production from the thermal way is located only where the temperature is over 2000K at the flame end.

## VII.Conclusions

A lean premixed burner prototype was designed and investigated. The prototype was derived from an existing DLN industrial unit where a new swirler reinforces the internal recirculation zone. Moreover, the units it was equipped with a new movable fuel injection system to allow the controlling of the mixing and the flame flashback.

The burner was tested at atmospheric combustion test facility with 100% hydrogen fueling; this activity confirmed the operability with pure Hydrogen. The operative points present a higher outlet velocity than the natural gas operation, from 80m/s to 130m/s.

The experimental campaign was addressed to measure the NO<sub>x</sub> emissions and flashback limits and two configurations were investigated. The best arrangement regarding NO<sub>x</sub> emissions is the case with nominal premix level and without the pilot. It showed a range of NO<sub>x</sub> emission from 5 to 17 ppm@15%O<sub>2</sub>, for equivalence ratio varying from 0.25 to 0.34.

The main issue of the unit regards the burner pressure drop, values from 3.3 up to 6% were measured. The higher value was related to the configuration with higher premixing, i.e. low emission, which requires for higher velocity flow. The numerical activity permits to understand the early ignition of the fuel and how it influences the operability.

The chemical post processor shows the importance of NNH path in the NO<sub>x</sub> emissions when the flame presents an early ignition, only the 20% of NO<sub>x</sub> emission is attributed to Zeldovic mechanism.

This result is important because the using of premixing technology is a historical solution, in hydrocarbon fueling, to reduce the temperature in the combustion chamber thus to reduce the NO emission. In 100% hydrogen fueling this technology is opposed by hydrogen promoted path thus the final result is a reduction of wished effect.

## VIII.Acknowledgments

Authors want to acknowledge Giovanni Riccio, Alessandro Marini, Iarno Brunetti and Stefano Sigali. This work was conducted as part of the project "Sviluppo di un combustore ultra low NO<sub>x</sub> per idrogeno" (2011-2013). The authors wish to thank the Regione Veneto (Italy) for supporting the project and ENEL as the coordinator of the project.

Alessandro Cappelletti, Francesco Martelli, Investigation of a pure hydrogen fueled gas turbine burner, International Journal of Hydrogen Energy, Available online 11 March 2017, ISSN 0360-3199, <http://dx.doi.org/10.1016/j.ijhydene.2017.02.104>.  
(<http://www.sciencedirect.com/science/article/pii/S0360319917306122>)

## References

- [1] Moriarty P, Honnery D. Hydrogen's role in an uncertain energy future. *Int J Hydrogen Energy* 2009;34:31–9. doi:10.1016/j.ijhydene.2008.10.060.
- [2] Ball M, Wietschel M. The future of hydrogen - opportunities and challenges. *Int J Hydrogen Energy* 2009;34:615–27. doi:10.1016/j.ijhydene.2008.11.014.
- [3] Gahleitner G. Hydrogen from renewable electricity: An international review of power-to-gas pilot plants for stationary applications. *Int J Hydrogen Energy* 2012;38:2039–61. doi:10.1016/j.ijhydene.2012.12.010.
- [4] Muangrat R. A review: utilization of food wastes for hydrogen production under hydrothermal gasification. *Environ Technol Rev* 2013:1–16. doi:10.1080/21622515.2013.840682.
- [5] Cormos C-C. Hydrogen and power co-generation based on coal and biomass/solid wastes co-gasification with carbon capture and storage. *Int J Hydrogen Energy* 2012;37:5637–48. doi:10.1016/j.ijhydene.2011.12.132.
- [6] Cormos C-C. Assessment of hydrogen and electricity co-production schemes based on gasification process with carbon capture and storage. *Int J Hydrogen Energy* 2009;34:6065–77. doi:10.1016/j.ijhydene.2009.05.054.
- [7] Brunetti I, Rossi N, Sigali S, Sonato G, Cocchi S. ENEL's Fusina zero emission combined cycle: experiencing hydrogen combustion. *POWERGEN Eur.*, 2010.
- [8] Lee MC, Yoon J, Joo S, Yoon Y. Gas turbine combustion characteristics of H<sub>2</sub>/CO synthetic gas for coal integrated gasification combined cycle applications. *Int J Hydrogen Energy* 2015;40:11032–45. doi:10.1016/j.ijhydene.2015.06.086.
- [9] Isfahani SNR, Sedaghat A. A hybrid micro gas turbine and solid state fuel cell power plant with hydrogen production and CO<sub>2</sub> capture. *Int J Hydrogen Energy* 2016;41:9490–9. doi:10.1016/j.ijhydene.2016.04.065.
- [10] Chinda P, Brault P. The hybrid solid oxide fuel cell (SOFC) and gas turbine (GT) systems steady state modeling. *Int J Hydrogen Energy* 2012;37:9237–48. doi:10.1016/j.ijhydene.2012.03.005.
- [11] Chiesa P, Lozza G, Mazzocchi L. Using Hydrogen as Gas Turbine Fuel. *J Eng Gas Turbines Power* 2005;127:73. doi:10.1115/1.1787513.
- [12] Cappelletti A, Martelli F, Bianchi E, Trifoni E. Numerical Redesign of 100kw MGT Combustor for 100% H<sub>2</sub> fueling. *Energy Procedia* 2014;45:1412–21. doi:10.1016/j.egypro.2014.01.148.
- [13] Sampath P. Combustion performance of hydrogen in a small gas turbine combustor. *Int J Hydrogen Energy* 1985;10:829–37. doi:10.1016/0360-3199(85)90172-7.
- [14] Nomura M, Tamaki H, Morishita T, Ikeda H, Hatori K. Hydrogen combustion test in a small gas turbine. *Int J Hydrogen Energy* 1981;6:397–412. doi:http://dx.doi.org/10.1016/0360-3199(81)90065-3.
- [15] Cocchi S, Provenzale M, Cinti V, Carrai L, Sigali S, Cappetti D. Experimental Characterization of a Hydrogen Fuelled Combustor With Reduced NO<sub>x</sub> Emissions for a 10 MW Class Gas Turbine. Vol 3 Combust Fuels Emiss Parts A B 2008:991–1000. doi:10.1115/GT2008-51271.
- [16] Riccio G, Marini A, Martelli F. Numerical investigations of gas turbine combustion chamber Hydrogen fired. *ISABE-2009-1112*, 2009.
- [17] Shelil N, Griffiths A, Bagdanavicius A, Syred N. Flashback Limits of Premixed H<sub>2</sub>/CH<sub>4</sub> Flames in a Swirl-Stabilized Combustor. Vol. 2 Combust. Fuels Emiss. Parts A B, vol. 2010, ASME; 2010, p. 1247–58. doi:10.1115/GT2010-23623.

Alessandro Cappelletti, Francesco Martelli, Investigation of a pure hydrogen fueled gas turbine burner, *International Journal of Hydrogen Energy*, Available online 11 March 2017, ISSN 0360-3199, <http://dx.doi.org/10.1016/j.ijhydene.2017.02.104>.  
(<http://www.sciencedirect.com/science/article/pii/S0360319917306122>)

- [18] Kwon OC, Faeth GM. Flame/stretch interactions of premixed hydrogen-fueled flames: measurements and predictions. *Combust Flame* 2001;124:590–610. doi:[http://dx.doi.org/10.1016/S0010-2180\(00\)00229-7](http://dx.doi.org/10.1016/S0010-2180(00)00229-7).
- [19] Rozenchan G, Zhu DL, Law CK, Tse SD. Outward propagation, burning velocities, and chemical effects of methane flames up to 60 ATM. *Proc Combust Inst* 2002;29:1461–70. doi:10.1016/S1540-7489(02)80179-1.
- [20] Pareja J, Burbano HJ, Amell A, Carvajal J. Laminar burning velocities and flame stability analysis of hydrogen/air premixed flames at low pressure. *Int J Hydrogen Energy* 2011;36:6317–24. doi:10.1016/j.ijhydene.2011.02.042.
- [21] Noble DR, Zhang Q, Shareef A, Tootle J, Meyers A, Lieuwen T. Syngas Mixture Composition Effects Upon Flashback and Blowout. Vol. 1 *Combust. Fuels, Educ.*, vol. 2006, ASME; 2006, p. 357–68. doi:10.1115/GT2006-90470.
- [22] Schönborn A, Sayad P, Konnov AA, Klingmann J. OH\*-chemiluminescence during autoignition of hydrogen with air in a pressurised turbulent flow reactor. *Int J Hydrogen Energy* 2014;39:12166–81. doi:10.1016/j.ijhydene.2014.05.157.
- [23] Burmberger S, Hirsch C, Sattelmayer T. Designing a Radial Swirler Vortex Breakdown Burner. Vol 1 *Combust Fuels, Educ* 2006:423–31. doi:10.1115/GT2006-90497.
- [24] Therkelsen P, Werts T, McDonell V, Samuelson S. Analysis of NO<sub>x</sub> Formation in a Hydrogen-Fueled Gas Turbine Engine. *J Eng Gas Turbines Power* 2009;131:31507. doi:10.1115/1.3028232.
- [25] Hernandez SR, Wang Q, McDonell VG, Mansour A, Steinhilber E, Hollon B. Micro-mixing fuel injectors for low emissions hydrogen combustion. *ASME Turbo Expo 2008 Power Land, Sea Air* 2008. doi:10.1115/GT2008-50854.
- [26] York WD, Ziminsky WS, Yilmaz E. Development and Testing of a Low NO<sub>x</sub> Hydrogen Combustion System for Heavy-Duty Gas Turbines. *J Eng Gas Turbines Power* 2013;135:22001. doi:10.1115/1.4007733.
- [27] Marek C, Smith T, Kundu K. Low Emission Hydrogen Combustors for Gas Turbines Using Lean Direct Injection. 41st AIAA/ASME/SAE/ASEE Jt. Propuls. Conf. & Exhib., Reston, Virginia: American Institute of Aeronautics and Astronautics; 2005, p. 1–27. doi:10.2514/6.2005-3776.
- [28] Brunetti I, Riccio G, Rossi N, Cappelletti A, Bonelli L, Marini A, et al. Experimental and Numerical Characterization of Lean Hydrogen Combustion in a Premix Burner Prototype. Vol 2 *Combust Fuels Emiss Parts A B* 2011;2011:601–12. doi:10.1115/GT2011-45623.
- [29] Galletti C, Parente a., Derudi M, Rota R, Tognotti L. Numerical and experimental analysis of NO emissions from a lab-scale burner fed with hydrogen-enriched fuels and operating in MILD combustion. *Int J Hydrogen Energy* 2009;34:8339–51. doi:10.1016/j.ijhydene.2009.07.095.
- [30] Schoepflin L, Riccio G, Adami P, Martelli F. Studio dell'iniezione di H<sub>2</sub> in sistemi di premiscelamento. *ATI* 2006, 2006.
- [31] Riccio G, Schoepflin L, Adami P, Martelli F. Analysis of the Fuel Injection in Gas Turbine Premixing Systems by Experimental Correlations and Numerical Simulations. Vol. 1 *Combust. Fuels, Educ.*, vol. 2006, ASME; 2006, p. 123–35. doi:10.1115/GT2006-90174.
- [32] Gobbato P, Masi M, Cappelletti A, Antonello M. Effect of the Reynolds number and the basic design parameters on the isothermal flow field of low-swirl combustors. *Exp Therm Fluid Sci* 2017. doi:10.1016/j.expthermflusci.2017.02.001.
- [33] LILLEY DG. Swirling flows in typical combustor geometries. *J Propuls Power* 1986;2:64–72. doi:10.2514/3.22846.

Alessandro Cappelletti, Francesco Martelli, Investigation of a pure hydrogen fueled gas turbine burner, *International Journal of Hydrogen Energy*, Available online 11 March 2017, ISSN 0360-3199, <http://dx.doi.org/10.1016/j.ijhydene.2017.02.104>.  
(<http://www.sciencedirect.com/science/article/pii/S0360319917306122>)

- [34] Therkelsen P, Mauzey J, McDonell V, Samuelsen S. Evaluation of a Low Emission Gas Turbine Operated on Hydrogen. Vol. 1 Combust. Fuels, Educ., vol. 2006, ASME; 2006, p. 557–64. doi:10.1115/GT2006-90725.
- [35] Cerutti M, Cocchi S, Modi R, Sigali S, Bruti G. Hydrogen Fueled Dry Low NOx Gas Turbine Combustor Conceptual Design. Vol. 4B Combust. Fuels Emiss., ASME; 2014, p. V04BT04A014. doi:10.1115/GT2014-26136.
- [36] Tiribuzi S. CFD Modelling of Thermoacoustic Oscillations Inside an Atmospheric Test Rig Generated by a DLN Burner. Vol 1 Turbo Expo 2004 2004;2004:475–85. doi:10.1115/GT2004-53738.
- [37] Cipriano A, Gasperetti S, Mariotti G, Paganini E. Analysis of the Spectral Properties of Premixed, Diffusion, and Hybrid Natural Gas Flames. Vol 1 Turbo Expo 2004 2004:313–20. doi:10.1115/GT2004-53506.
- [38] Kaskan WE. The dependence of flame temperature on mass burning velocity. *Symp Combust* 1957;6:134–43. doi:10.1016/S0082-0784(57)80021-6.
- [39] Gobbato P, Masi M, Toffolo A, Lazzaretto A. Numerical simulation of a hydrogen fuelled gas turbine combustor. *Int J Hydrogen Energy* 2011;36:7993–8002. doi:10.1016/j.ijhydene.2011.01.045.
- [40] Zimont V, Polifke W, Bettelini M, Weisenstein W. An Efficient Computational Model for Premixed Turbulent Combustion at High Reynolds Numbers Based on a Turbulent Flame Speed Closure. *J Eng Gas Turbines Power* 1998;120:526. doi:10.1115/1.2818178.
- [41] Zimont VL. Gas premixed combustion at high turbulence. Turbulent flame closure combustion model. *Exp Therm Fluid Sci* 2000;21:179–86. doi:10.1016/S0894-1777(99)00069-2.
- [42] Peters N. Laminar flamelet concepts in turbulent combustion. *Symp Combust* 1988;21:1231–50. doi:10.1016/S0082-0784(88)80355-2.
- [43] Peters N. The turbulent burning velocity for large-scale and small-scale turbulence. *J Fluid Mech* 1999;384:107–32. doi:10.1017/S0022112098004212.
- [44] Göttgens J, Mauss F, Peters N. Analytic approximations of burning velocities and flame thicknesses of lean hydrogen, methane, ethylene, ethane, acetylene, and propane flames. *Symp Combust* 1992;24:129–35. doi:10.1016/S0082-0784(06)80020-2.
- [45] Gobbato P, Masi M, Toffolo A, Lazzaretto A. Numerical simulation of a hydrogen fuelled gas turbine combustor. *Int J Hydrogen Energy* 2011;36:7993–8002. doi:10.1016/j.ijhydene.2011.01.045.
- [46] Andreini A, Da Soghe R, Facchini B, Mazzei L, Colantuoni S, Turrini F. Local Source Based CFD Modeling of Effusion Cooling Holes: Validation and Application to an Actual Combustor Test Case. *J Eng Gas Turbines Power* 2013;136:11506. doi:10.1115/1.4025316.
- [47] Da Soghe R, Bianchini C, Andreini A, Mazzei L, Riccio G, Marini A, et al. Thermofluid Dynamic Analysis of a Gas Turbine Transition-Piece. *J Eng Gas Turbines Power* 2015;137:62602. doi:10.1115/1.4028869.
- [48] Li J, Zhao Z, Kazakov A, Dryer FL. An updated comprehensive kinetic model of hydrogen combustion. *Int J Chem Kinet* 2004;36:566–75. doi:10.1002/kin.20026.
- [49] Li J, Zhao Z, Kazakov A, Chaos M, Dryer FL, Scire JJ. A Comprehensive Kinetic Mechanism for CO, CH<sub>2</sub>O, and CH<sub>3</sub>OH Combustion. *Int J Chem Kinet* 2007. doi:10.1002/kin.20218.
- [50] Ströhle J, Myhrvold T. An evaluation of detailed reaction mechanisms for hydrogen combustion under gas turbine conditions. *Int J Hydrogen Energy* 2007;32:125–35. doi:10.1016/j.ijhydene.2006.04.005.
- [51] ANSYS FLUENT User's Guide. 2013.
- [52] ANSYS. ANSYS FLUENT Theory Guide 2013.



Alessandro Cappelletti, Francesco Martelli, Investigation of a pure hydrogen fueled gas turbine burner, International Journal of Hydrogen Energy, Available online 11 March 2017, ISSN 0360-3199, <http://dx.doi.org/10.1016/j.ijhydene.2017.02.104>.  
(<http://www.sciencedirect.com/science/article/pii/S0360319917306122>)

- [53] Ansys. ANSYS Fluid Dynamics Verification Manual 2013.
- [54] Marini A, Cappelletti A, Riccio G, Martelli F. Cfd re-design of a gas turbine can-type combustion chamber hydrogen fired. ECCOMAS CFD 2010, June 14-17, Lisbon, Port., 2010.
- [55] Cappelletti A, Insinna M, Martelli F. Numerical Simulation of Wet Combustion to Control NOx Emissions of a Heavy-Duty Gas Turbine Combustor. 22nd Int. Symp. Air Breath. Engines, Oct. 25-30, 2015, Phoenix, Arizona., Phoenix, Arizona: 2015.
- [56] Montomoli F, Insinna M, Cappelletti A, Salvadori S. Uncertainty Quantification and Stochastic Variations of Renewable Fuels. Vol. 4B Combust. Fuels Emiss., Montréal, Canada: ASME; 2015, p. V04BT04A010. doi:10.1115/GT2015-43190.
- [57] Skottene M, Rian KE. A study of NOx formation in hydrogen flames. Int J Hydrogen Energy 2007;32:3572–85. doi:10.1016/j.ijhydene.2007.02.038.
- [58] MILLER J, BRANCH M, KEE R. A chemical kinetic model for the selective reduction of nitric oxide by ammonia. Combust Flame 1981;43:81–98. doi:10.1016/0010-2180(81)90008-0.
- [59] Bozzelli JW, Dean AM. O + NNH: A possible new route for NOx formation in flames. Int J Chem Kinet 1995;27:1097–109. doi:10.1002/kin.550271107.
- [60] Smith GP, Golden DM, Frenklach M, Moriarty NW, Eiteneer B, Goldenber M, et al. GRI-MECH 3.0 n.d.:[http://www.me.berkeley.edu/gri\\_mech/](http://www.me.berkeley.edu/gri_mech/).
- [61] Konnov A., De Ruyck J. Temperature-dependent rate constant for the reaction  $\text{NNH} + \text{O} \rightarrow \text{NH} + \text{NO}$ . Combust Flame 2001;125:1258–64. doi:10.1016/S0010-2180(01)00250-4.
- [62] Biagioli F, Güthe F. Effect of pressure and fuel–air unmixedness on NOx emissions from industrial gas turbine burners. Combust Flame 2007;151:274–88. doi:10.1016/j.combustflame.2007.04.007.
- [63] GUO H, NEILL W. A numerical study on the effect of hydrogen/reformate gas addition on flame temperature and NO formation in strained methane/air diffusion flames. Combust Flame 2009;156:477–83. doi:10.1016/j.combustflame.2008.07.009.
- [64] CentaurSoft. Centaur 2011:<http://www.centaursoft.com/>.
- [65] Guo H, Smallwood GJ, Liu F, Ju Y, Gülder ÖL. The effect of hydrogen addition on flammability limit and NOx emission in ultra-lean counterflow CH4/air premixed flames. Proc Combust Inst 2005;30:303–11. doi:10.1016/j.proci.2004.08.177.

### Figure caption

Figure 1: Schematic drawing of the burner prototype

Figure 2: Combustion chamber section view

Figure 3: Temperature Profile: Measured Value Vs Corrected Value

Figure 4: 3-D geometric model of the premixer

Figure 5: Equivalence ratio effect on non-dimensional temperature profile

Figure 6: A) Outlet velocity [m/s] effect on non-dimensional temperature profile, over 100 m/s cases, B) Average non-dimensional temperature profile (bottom)

Figure 7: A) Outlet velocity [m/s] effect on non-dimensional temperature profile, lower 100 m/s cases, B) Average non-dimensional temperature profile (bottom)

Figure 8: A) NO<sub>x</sub> emission Vs Thermal Input, B) NO<sub>x</sub> emission Vs Outlet velocity

Figure 9: A) Non-dimensional temperature profile. Exp Vs CFD B) CFD Temperature [K] field on longitudinal plane

Figure 10: OH\* Exp. Image Vs Premix-C Rate from CFD

Figure 11: The complete CFD image of Premix - C rate on a longitudinal plane

Figure 12: A) Iso surface of rate NO thermal B) Iso surface of rate NO via NNH, value  $10^{-5}$  kgmol/m<sup>3</sup>s

### Figures

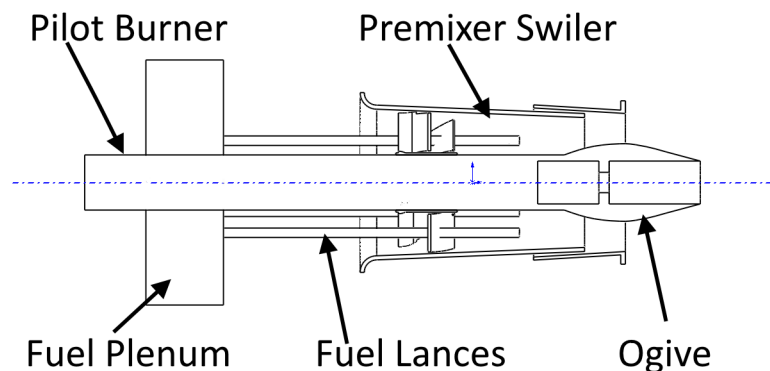


Figure 1

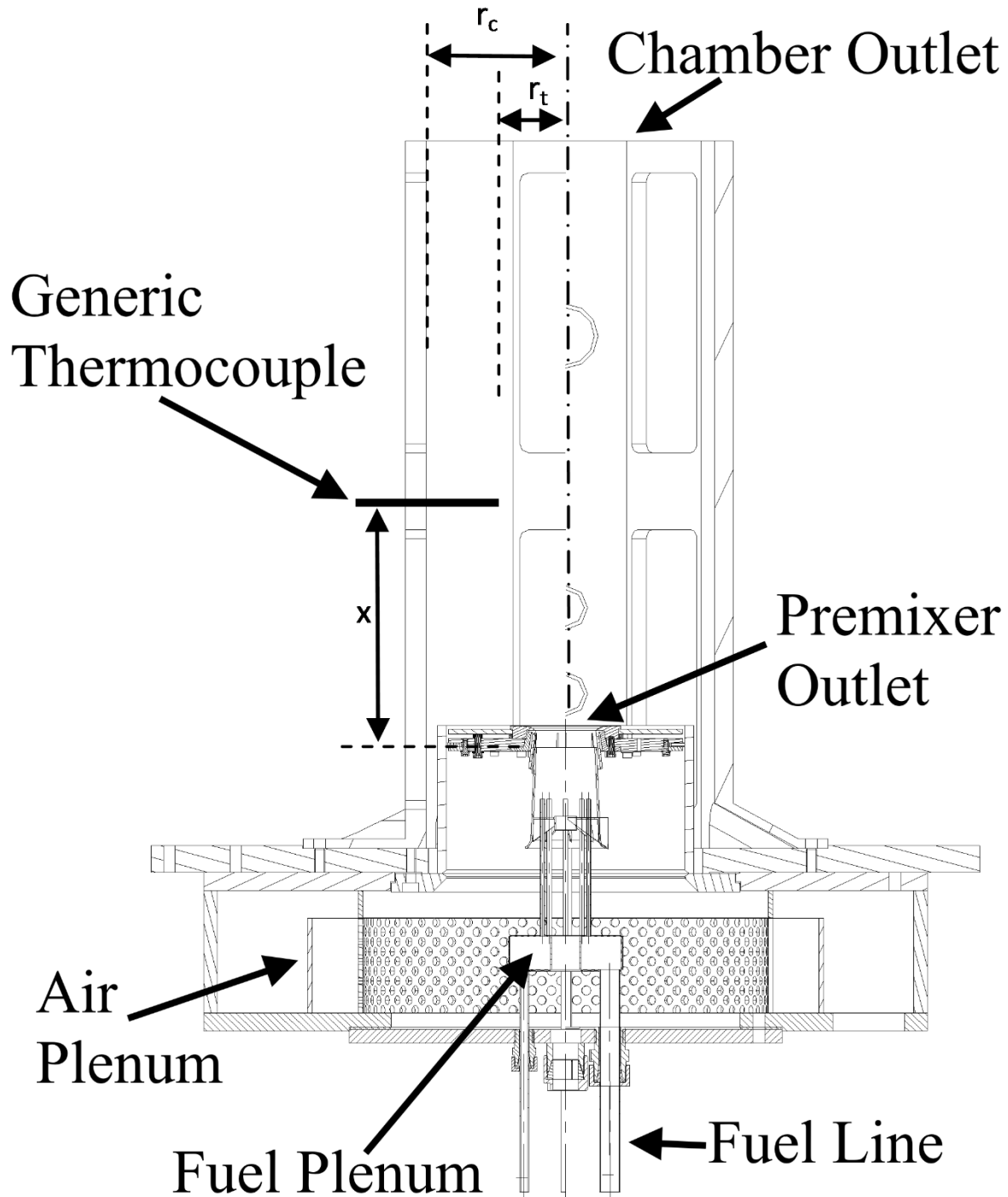


Figure 2

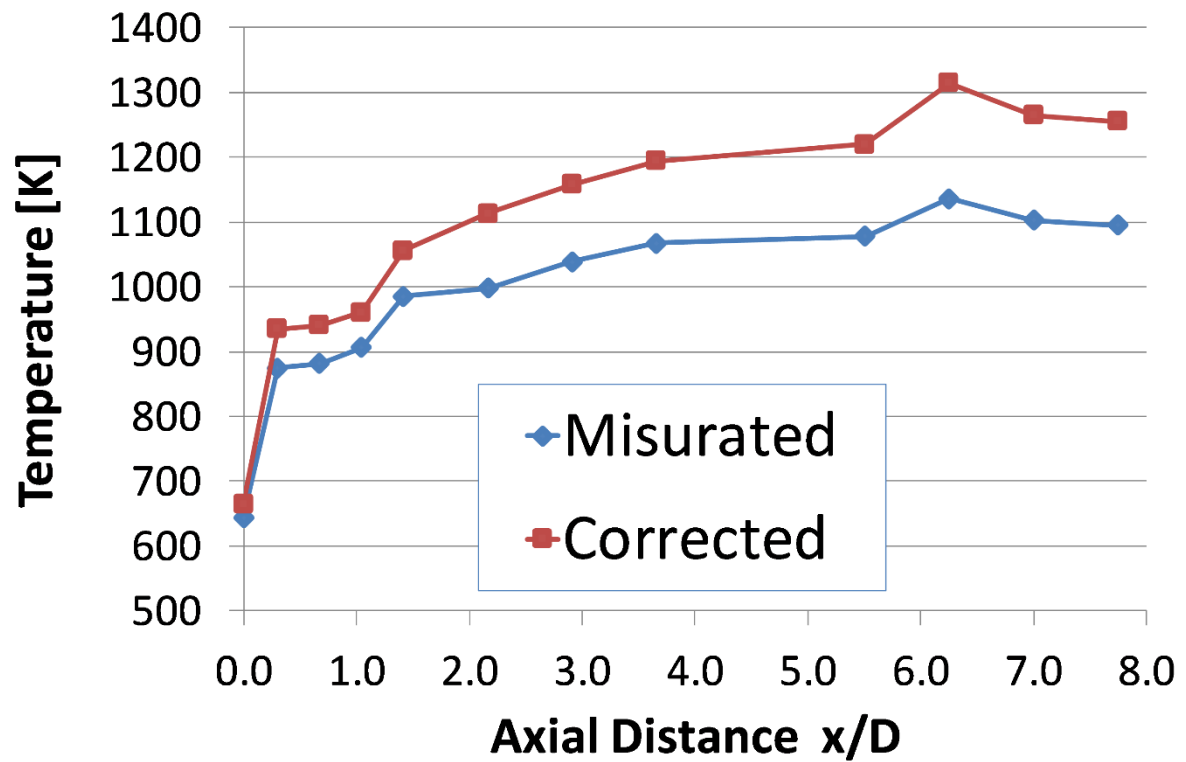


Figure 3

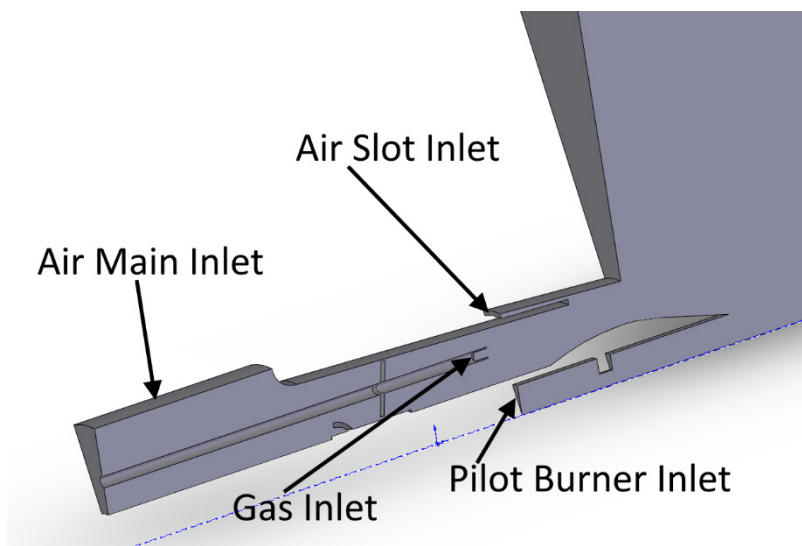


Figure 4

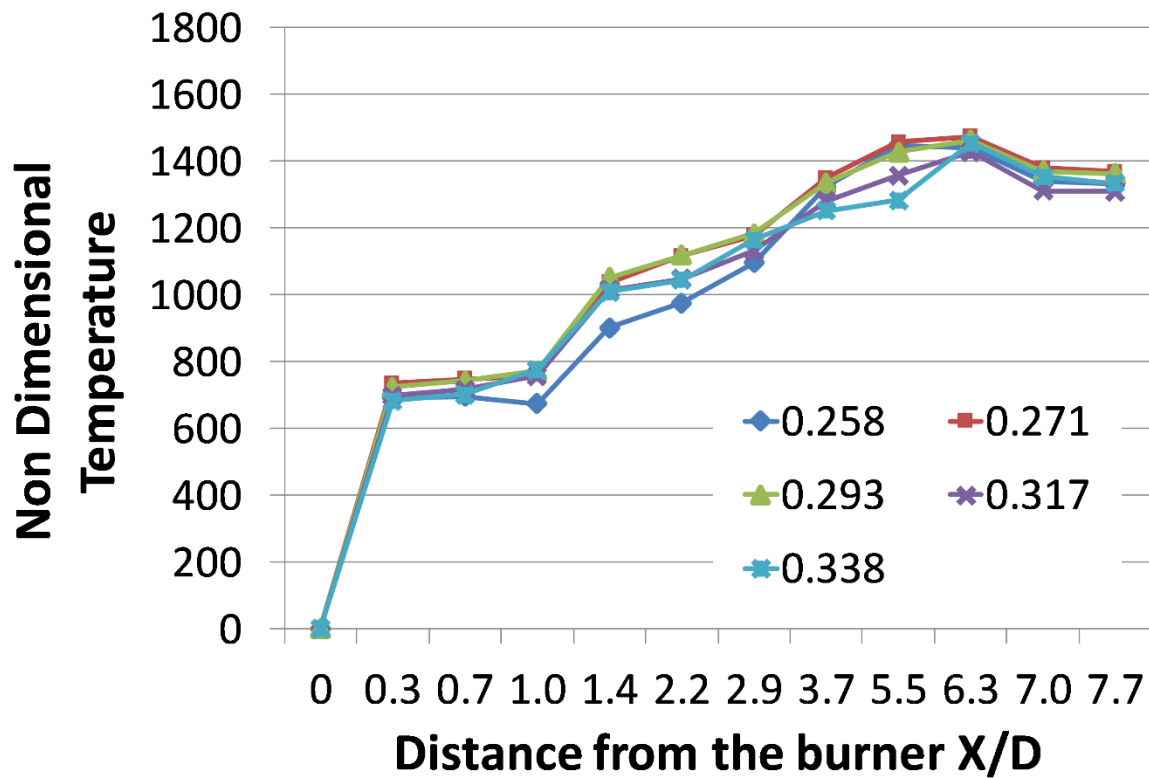


Figure 5

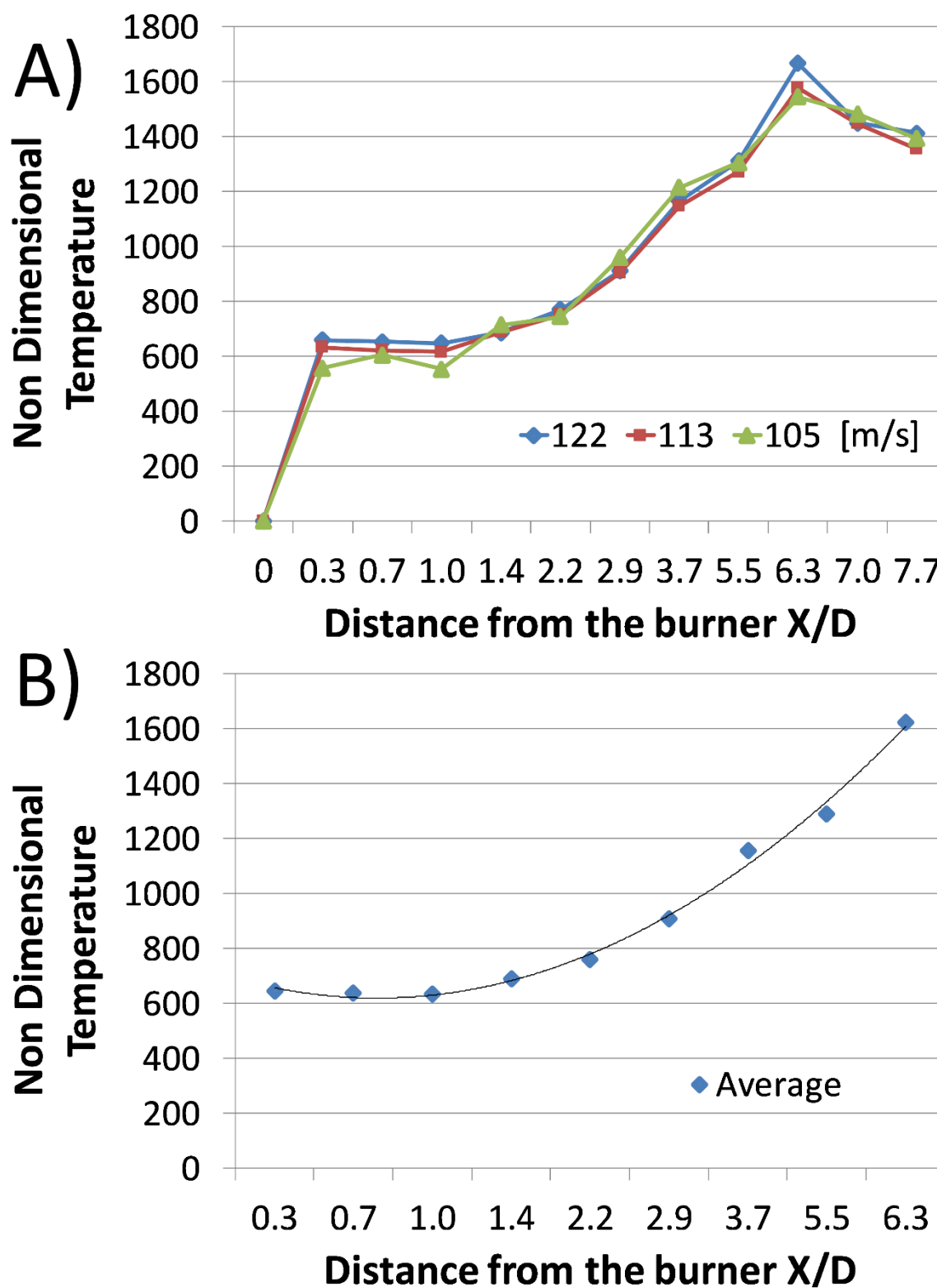


Figure 6

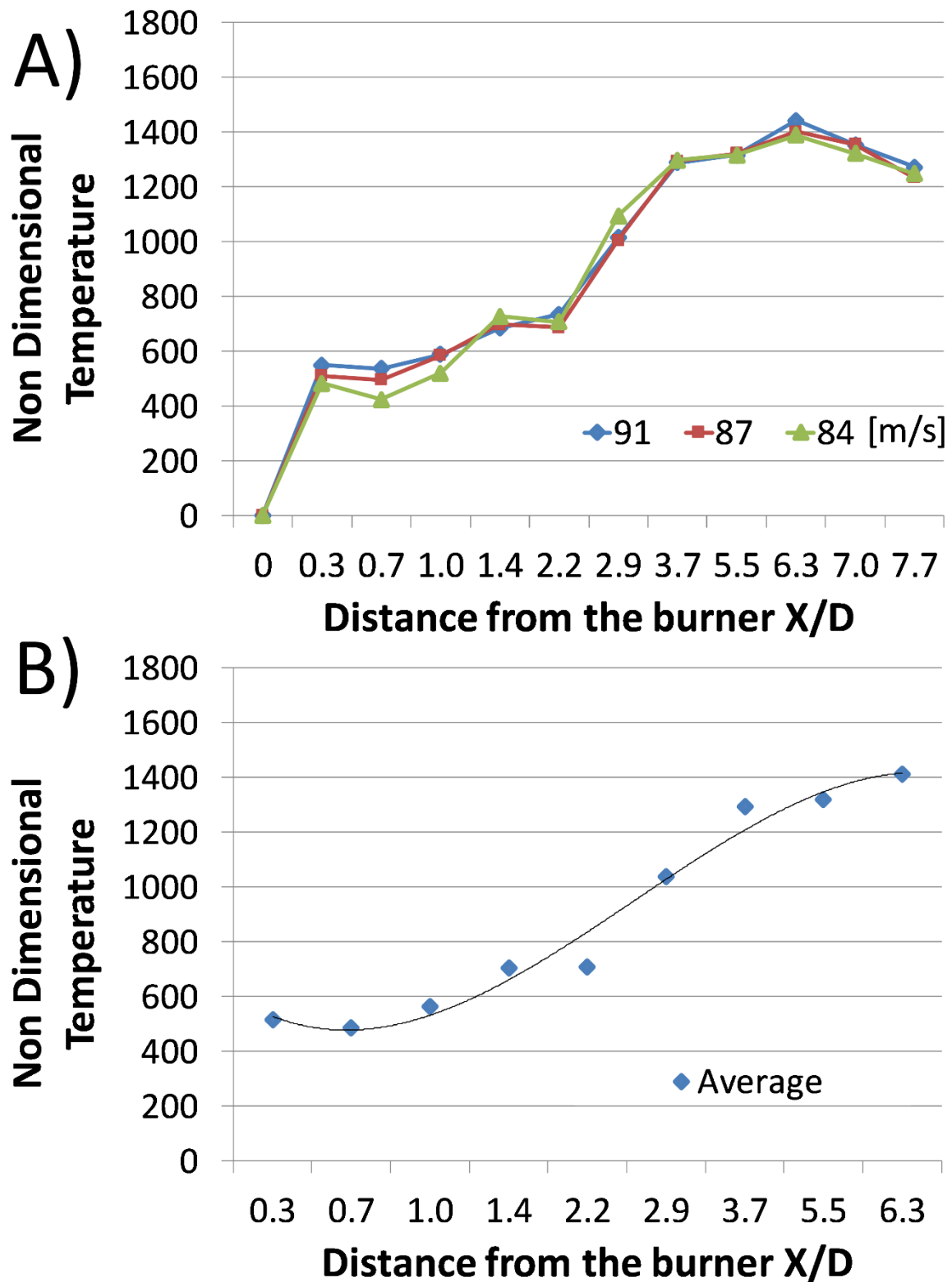


Figure 7

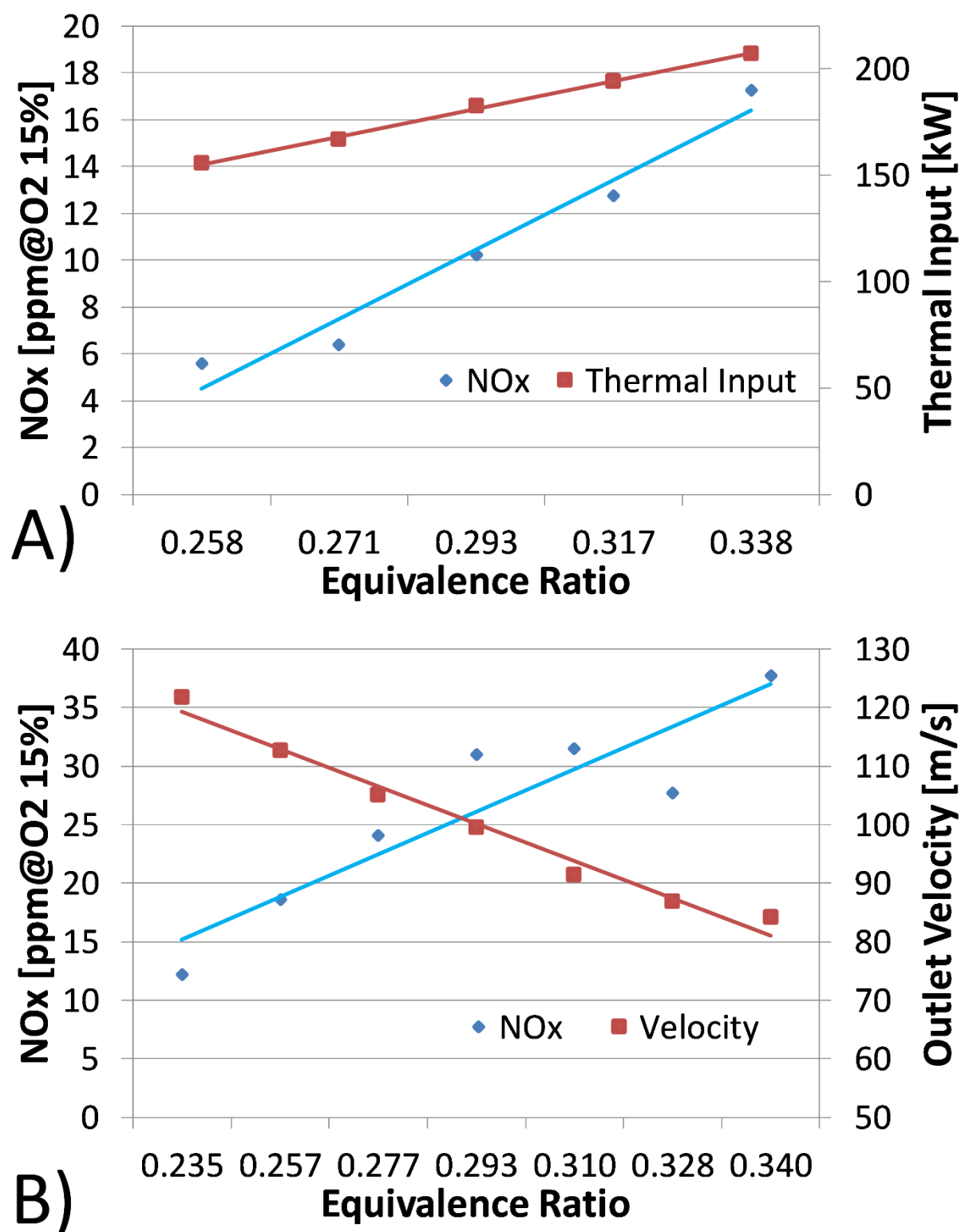


Figure 8



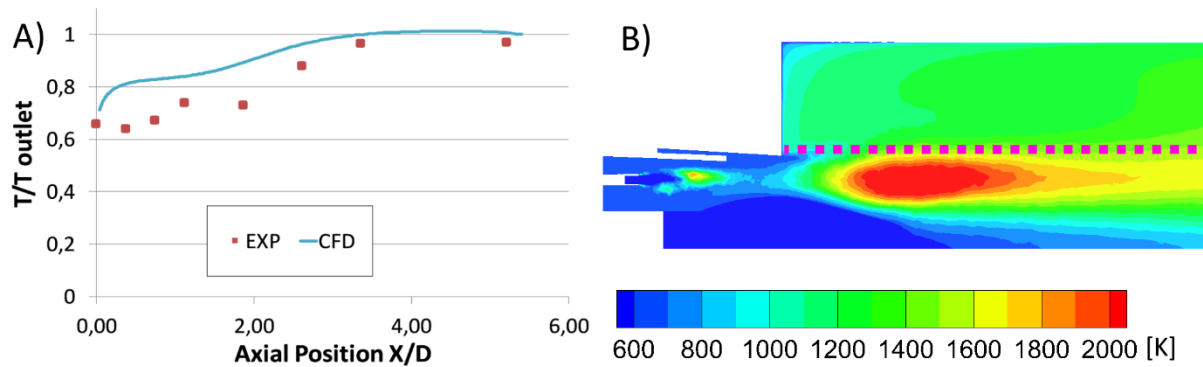


Figure 9

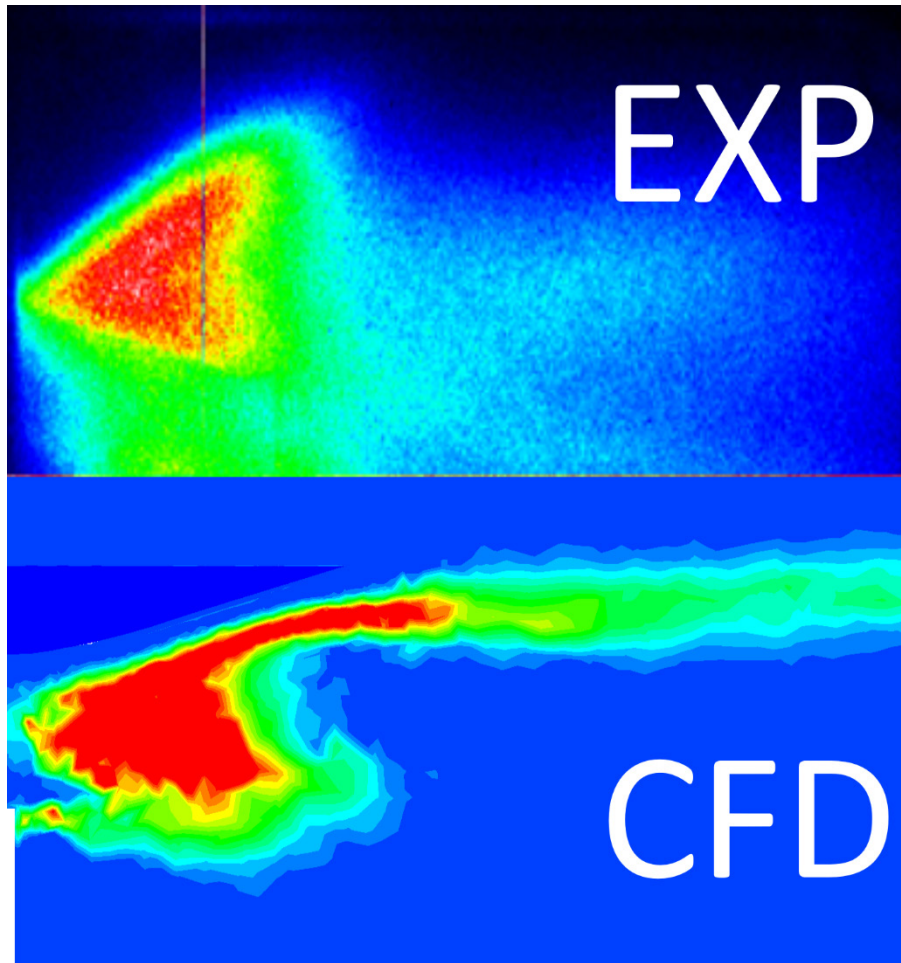


Figure 10

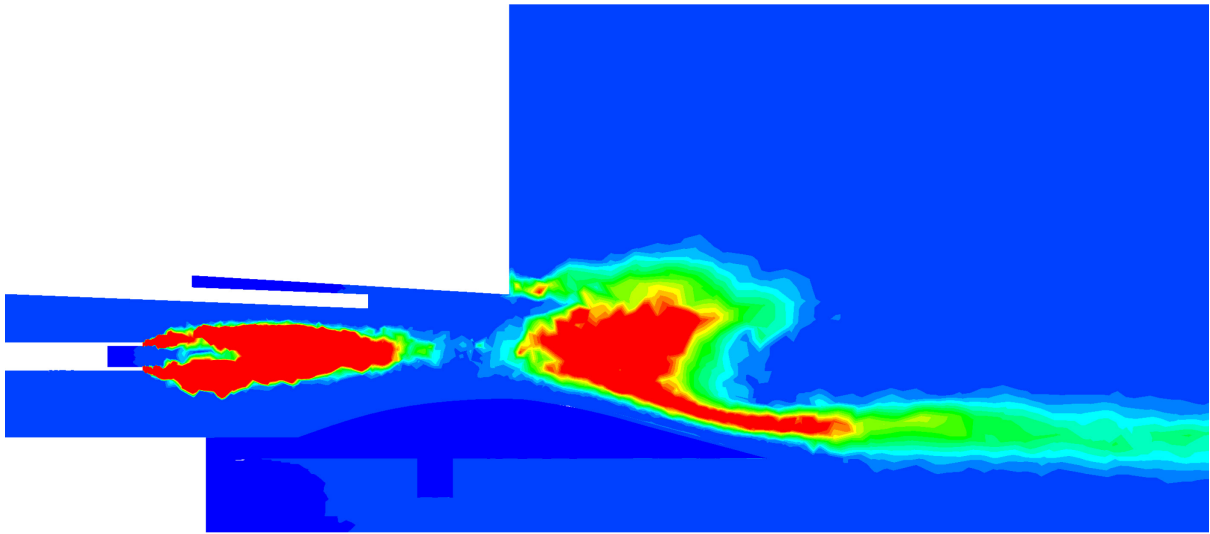


Figure 11

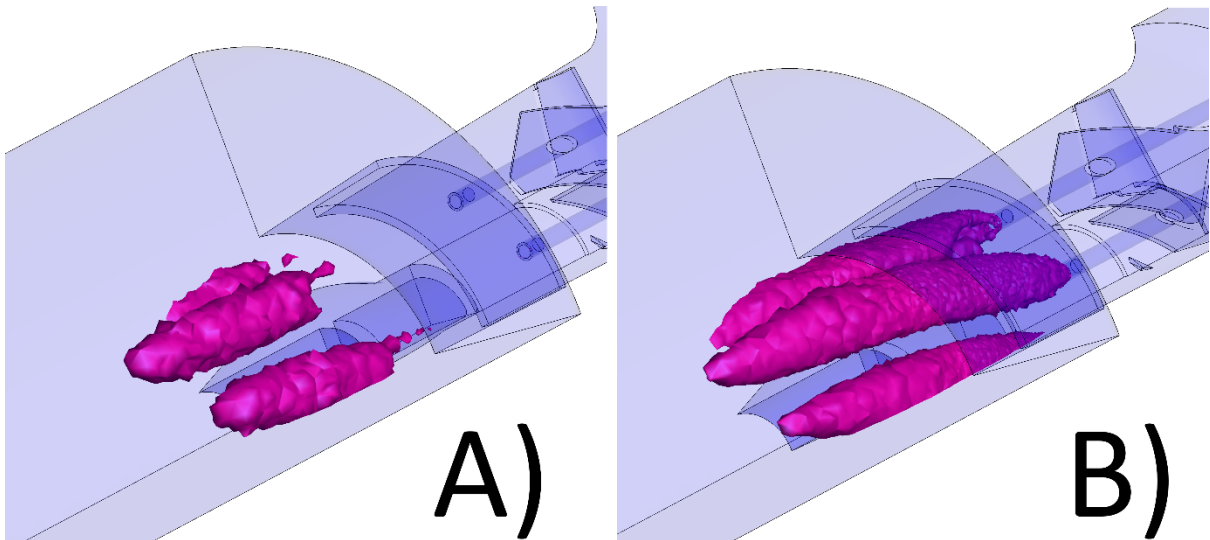


Figure 12

Alessandro Cappelletti, Francesco Martelli, Investigation of a pure hydrogen fueled gas turbine burner, International Journal of Hydrogen Energy, Available online 11 March 2017, ISSN 0360-3199, <http://dx.doi.org/10.1016/j.ijhydene.2017.02.104>.  
(<http://www.sciencedirect.com/science/article/pii/S0360319917306122>)

### Tables Captions

Table 1: Operation parameters range for 100% H<sub>2</sub> firing

Table 2: Flash-back speed limit and burner pressure drop

Table 3: Boundary conditions

Table 4 : Evaluation NO emission, Exp. Vs CFD

### Tables

Working pressure	atm	1
Premixer air temperature	°C	380
Premixer thermal load	kW	120-206
Premixer discharge velocity (with ogive)	m/s	80-130
Premixer equivalence ratio " $\phi$ "	-	0.29- 0.35

Table 1

Configuration	Flash-back speed limit [m/s]	Pressure drop [%]
Nominal	127	6.0
Low premix	87	3.3

Table 2

Working pressure	atm	1
Premixer airflow rate	g/s	113
Premixer air temperature	K	663

Alessandro Cappelletti, Francesco Martelli, Investigation of a pure hydrogen fueled gas turbine burner, International Journal of Hydrogen Energy, Available online 11 March 2017, ISSN 0360-3199, <http://dx.doi.org/10.1016/j.ijhydene.2017.02.104>.  
(<http://www.sciencedirect.com/science/article/pii/S0360319917306122>)

<b>Premixer thermal load</b>	kW	132
<b>Premixer discharge velocity (with ogive)</b>	m/s	84
<b>Premixer nominal overall equivalence ratio "<math>\phi</math>"</b>	-	0.340
<b>Experimental NO emission</b>	ppm@15% O <sub>2</sub>	38

Table 3

	ppm NO @15% O <sub>2</sub>
Experimental	38.00
Pure Thermal Postprocessor	9.59
Decoupled only Thermal way	6.32
Decoupled All ways	41.00

Table 4